Indian Journal of Traditional Knowledge
Vol 22(4), October 2023, pp 727-738
DOI: 10.56042/ijtk.v22i4.7196

Preclinical pharmacokinetics and herb-drug interaction studies of atorvastatin co-administered with the herbal slimming products

Athar Husain[a,c], Mohammad Irshad Reza[a], Shailesh D Dagde[a], Syed Anees Ahmed[a,c], Pragati Singh[a], Saurabh Verma[a,c], Roshan Katekar[a,c], Ashish Kumar[a] & Jiaur R Gayen[a,b,c,*]

[a]Pharmaceutics & Pharmacokinetics Division, [b]Pharmacology Division, CSIR-Central Drug Research Institute, Lucknow 226 031, India
[c]Academy of Scientific and Innovative Research (AcSIR), Ghaziabad 201 002 India

[*]E-mail: jr.gayen@cdri.res.in

Received 08 October 2021; revised 17 February 2022; accepted 06 April 2022

Herbal slimming products (HSPs) contain multiple herbs used in weight loss. Phytoconstituents of several plant extracts show the inhibitory effects on the drug-metabolizing enzymes causing interaction when taken with other drugs. Atorvastatin (ATS) is used in the treatment of hyperlipidemia. This study aimed to investigate the effect of HSPs on the pharmacokinetics and pharmacodynamics of ATS. ATS (10 mg/Kg) was administered alone or in combination with HSP1 (200 mg/Kg)/ HSP2 (165 mg/Kg) orally in the SD rats for pharmacokinetics study. Hyperlipidemia was induced in Golden Syrian Hamster by feeding HFD (60% kcal). Furthermore, biochemical levels in serum, ROS, gene expression and lipid accumulation levels were examined in hamster liver tissue. HSPs have significantly enhanced the permeability and inhibited the metabolism of ATS by inhibiting the CYP3A4 isoenzyme confirmed by *in vitro* assay. Co-administration of HSPs with ATS enhanced the relative bioavailability of ATS.Concomitant administration of HSPs with ATS has significantly reduced the fat content, inflammatory cytokines, TG, VLDL, LDL levels, tissue MDA level, HMGCR and SREBP1c mRNA expression levels, lipid accumulation as well as collagen content and has increased the serum HDL level as well as tissue SOD, CAT, GHS and mRNA expression levels of LXRα and CYP7A1. The aforementioned outcomes indicated that co-administration of HSPs with ATS may lead to herb-drug interaction. Therefore, precaution should be taken and dose adjustment is required when administered simultaneously.

Keywords: Atorvastatin, Cytochrome P450, Herb-drug interaction, HSPs, Metabolism

IPC Code: Int Cl.[23]: A61K 36/00, A61K 38/00, A61K 45/00

One of the ultimate vital causes of morbidity and mortality is drug interactions (DIs) in health care. Annually, over 2 million cases of DIs are reported, and approx. 1,00,000 death occurred due to medication errors[1]. The most common cause of DIs is an error in medication or polytherapy, which induces adverse drug reactions or decreases clinical efficacy[2]. Co-administration with other drugs can lead to side effects and alter the pharmacological response. The responses may be synergistic or antagonistic, dependent on whether the interaction is positive or negative. It can occur at any pharmacokinetics (PK) and pharmacodynamics (PD) level. Cytochrome P450 (CYP450) shows a crucial part in drug metabolism. Potent induction or inhibition of CYP3A4, CYP2D6, CYP2C19, CYP2C9 and CYP1A2 isoenzymes could lead to drug interaction and safety issues. CYPs enzymes are responsible for 90% metabolism of all marketed drugs[3]. Various anti-hyperlipidemic drugs are available in the market, but their prolonged use and drug interactions can lead to adverse effects. Atorvastatin (ATS) is an HMGCR (3-hydroxy-3-methyl-glutaryl-CoA reductase) inhibitor, extensively used in hyperlipidemia and metabolized by CYP3A4 isoenzyme[4].

Medicinal plants play an important role in drug discovery and development[5]. Approximately 70% of the world's rural population uses traditional medicines for their health care. Over the past 20 years, both developed and developing countries have used medicinal herbs as an alternative or complementary medicine. There is a belief about herbal medicine that it has little or no toxic effect because it is derived from natural resources; this is one of the reasons for increasing day-to-day consumption of herbal medicines worldwide. However, the safety and efficacy of most herbal medicines are not established due to limited scientific evidence[6]. Natural products

*Correspondence author

have multi-target effects because they contain a variety of mixtures of bioactive chemicals. Nevertheless, it has shown promising results due to polypharmacological profiles as well as disease-modifying properties[7].

Several herbal medicines cause interactions when taken with synthetic drugs. The herbal slimming product 1 (HSP1) contains *Babul, Guggul, Kutki, Haritaki, Indian gooseberry etc.,* whereas HSP2 contains *Guggul, Gurmar, Haritaki* and *Brindall Berry etc.* used in the weight loss. The phytoconstituents of HSPs can leads to herb-drug interaction by inhibiting the drug-metabolizing enzymes, *i.e.*, CYP450. Obese patients often use slimming products (HSPs) without consulting a registered medical practitioner. Until today no scientifically validated data are available regarding the combined use of the ATS and HSPs (HSP1 and HSP2). No studies have been conducted to scientifically evaluate the effect of HSP1 and HSP2 on the PK-PD parameters of ATS. Thus, it is logical to rationalize it to focus on the studies of metabolic pathways, inhibition and induction, and the drug interaction studies to explore its safety and interactivity potential for long-term use with some important diagnostic applications. The primary aim of this study was to investigate the effect of HSPs on the pharmacokinetic and pharmacodynamic of ATS. There is little literature available for actual interaction studies, so this study will help clinicians.

Materials and Methods

Chemicals and reagents

Atorvastatin (ATS), phenacetin (PHEN), phenol red, NADPH, testosterone, chlorzoxazone, diclofenac, dextromethorphan, bupropion HCl, coumarin, 6α-hydroxychlorzoxazone, dextrorphan, 5-hydroxyomeprazole, 4'-hydroxydiclofenac, 6-hydroxybupropion, 7- hydroxycoumarin, acetaminophen, sodium phosphate mono and dibasic, urethane, trisHCl, phenylmethylsulfonyl fluoride, and ethylenediaminetetraacetic acid (EDTA) disodium salt dehydrate were purchased from Sigma Aldrich. Tert-butyl methyl ether (TBME), ethyl acetate (EA) and acetonitrile (ACN) from Merck; ammonium acetate, formic acid, and magnesium chloride ($MgCl_2$) from SRL, 6β-hydroxytestosterone from Cayman; Sodium chloride, potassium chloride, and glycerol from Fisher Scientific; human liver microsome was obtained from BD Gentest. HSPs were purchased from the local market of Lucknow. Analytical grades of all chemicals and reagents were used in this study.

Animals

Sprague Dawley (SD) rats (male, 200-220 g) and Golden Syrian Hamster (male, 90-110 g) were used in this study. All animals were procured from the Division of Laboratory Animals of CSIR-CDRI, Lucknow, and acclimatized for one week before the experiment at standard condition (25±2°C and 55±5% RH). They were maintained under a 12 h light/dark cycle and received a standard diet and water *ad libitum*. CSIR-CDRI's Institutional Animal Ethics Committee (IAEC) has approved the experimental protocol (IEAC/2018/92).

Liquid Chromatographic and Mass Spectrometric conditions (LC-MS/MS)

QTRAP-4000 mass spectrometer (AB Sciex, Canada) equipped with ESI source was used for analysis. MRM (Multi reaction monitoring) was performed for quantification of ATS (559.28/440.1) and PHEN (180.2/110.2, IS) by monitoring the parent to product ion transition. The source and compound parameters of ATS and PHEN are listed in Table 1. Shimadzu UFLC system (Kyoto, Japan) equipped with SIL-HTcautosampler, LC-20AD binary pump, DGU-20A3 degasser, and CTO-20AC column oven was used to inject the sample. Phenomenex Luna (C18 (2), 100A, 75 x 4.6 mm, 3µ) column was used for chromatographic separation. Mobile phase A contains 0.1% formic acid in acetonitrile and mobile phase B containing ammonium acetate (10 mM) in a proportion of 80:20 (v/v) at the flow of 0.4 mL/min,

Table 1 — Compounds and source parameters of ATS and PHEN

Compound parameters	$[M+H]^+$ mode	
	ATS	PHEN (IS)
Parent ion (Q1)	559.28	180.2
Product ion (Q3)	440.1	110.2
Declustering potential (DP)	100	71
Entrance potential (EP)	10	10
Collision energy (CE)	30	30
Collision exit potential (CXP)	10	10
Source parameters		
Curtain gas (CUR)	30	
Collision gas (CAD)	High	
Ionspray voltage (ISV)	5500	
Temperature (ºC)	500	
Nebulizer gas (GS1)	40	
Auxiliary gas (GS2)	60	

were used for separation of ATS and PHEN. The dried residue was reconstituted with 100 µL of the mobile phase. During analysis, the column oven temperature was set at 40°C. 10 µL reconstituted sample was injected into the LC-MS/MS for quantification. The total run time was 5 min.

Calibration standard (CS) and quality control (QC) samples preparation

ATS was dissolved in Dimethyl sulfoxide (DMSO) while PHEN (IS for ATS) in methanol (MeOH) separately for making primary stock solutions (1 mg/mL). The concentration of CS working stocks for ATS were 10, 20, 50, 100, 200, 500, 1000, 2000, and 5000 ng/mL, while for QCs were 10, 30, 1890, 3750 ng/mL were prepared in ACN by serial dilution. QCs were prepared at four different concentration levels (LLOQ, LQC, MQC and HQC). 45 µL rat plasma and 5 µL of CS and/ QCs working stock were used for calibration curve as well as QCs samples to reach the final concentration 1, 2, 5, 10, 20, 50, 100, 200, and 500 ng/mL for CS, while 1, 3, 189, and 375 ng/mL for QCs.

Extraction procedure

ATS was extracted from rat plasma by applying protein precipitation followed by Liquid-liquid extraction. ACN containing IS (200 µL, PHEN 10 ng/mL) was added for the extraction of ATS from matrix plasma CS, QCs, plasma samples (50 µL), vortex for 20 sec and added 2 mL mixture of tert-butyl methyl ether (TBME) and ethyl acetate (EA) in the ratio of 50:50. Again vortex on multi-tube vortexed at 2000 rpm bench mixer (Benchmark) for 10 min, and centrifuged (Eppendorf) at 10000 rpm for 5 min at 25°C. Transferred the 1.5 mL of the supernatant into another clean ria vial tube. Nitrogen stream was used for drying the supernatant at 40°C. Dried residues were reconstituted with 100 µL mobile phase and 10 µL injected into the LC-MS/MS for quantification.

Bio-analytical assay method validation procedure

The LC-MS/MS bioanalytical ATS method was validated according to USFDA guidelines[8] regarding selectivity, recovery and matrix effect, linearity, precision and accuracy, carryover effect and dilution integrity[9].

Effect of HSPs on the permeability of ATS

Single-pass intestinal perfusion (SPIP) study was carried out as a formerly standardized method with some modification. Briefly, perfusion buffer (pH 7.2) was prepared by adding anhydrous sodium phosphate dibasic (5.77 g), sodium phosphate dehydrate monobasic (7.085 g), sodium chloride (7 g), adjusted volume with TDW up to 1 L[10]. Urethane (1.2 g per kg, i.p) was used to anaesthetize the overnight fasted rats. The intestinal segment (~10 cm) was exposed off by making the middle line incision in the abdomen (3-4 cm). Lumen was catheterized, connected with a perfusion pump and cleaned by using pre-warm normal saline. The desired concentration of ATS (1 µM) as well as zero permeability marker phenol red (PR, 28 µM), were co-perfused with and without HSPs (50 µg/mL) at a constant flow rate (0.2 mL/min). After 30 min, outlet perfusate was collected in 15 min intervals for 2 h. At the end of the experiment, without stretching, intestinal segment length was measured. Absorbance was taken at 558 nm for quantification of PR_{in} and PR_{out} perfusate. Effective permeability (P_{eff}) was calculated by using the following equations[11].

$$C_{out\ (corrected\ )} = C_{out} * \frac{PR_{in}}{PR_{out}}$$

$$P_{eff} = \frac{-Q_{in} \ln\left(\frac{C_{out\ (Corrected\ )}}{C_{in}}\right)}{2\pi rl}$$

Where, Q_{in} is the flow rate (0.2 mL/min), PR_{in} is the inlet and PR_{out} is the outlet concentration of phenol red, $C_{out\ (\text{corrected}\ )}$ is the outlet concentration of perfusate after correction, C_{in} is the entering of perfusate concentration, r is the intestine inner radius (0.18 cm), and l is the intestine length.

Microsomal stability study

Preparation of rat liver microsomes

Overnight fasted SD rats were anaesthetized by overexposure to Isoflurane. The liver was collected. 50 mM ice-cold tris-HCl buffer (pH 7.4) was used to remove the blood residue from the liver by washing it several times. The liver was softly blotted, weighed, chopped into tiny pieces, and homogenized using chilly homogenizing buffer [Sod. EDTA (1 mM), KCl (125 mM), and Tris-HCl (100 mM, pH 7.4)] in the ratio of 1:3 w/v. Centrifuged for 30 min at 9000 g (4°C). The supernatant was taken and again ultra-centrifuged at 4°C for 1 h at 100000 g. Resuspending buffer [Glycerol (20% v/v), Phenylmethylsulfonylfluoride (1 mM), Sod. EDTA (1 mM), Tris-HCl (100 mM, pH 7.4) and KCl (125 mM)] was used to resuspend the microsomal

pallet. Bradford method was used to estimate the protein's content using the Bovine serum albumin as standard and stored in -80°C for further study[12].

Metabolic stability study

In-vitro metabolic stability study was performed to assess the biotransformation of ATS (phase I reaction) in rat liver microsomes (RLM). *In-vitro* metabolic stability studies were conducted to determine the effect of HSPs on the metabolism of ATS (0.4 µM) in the presence and absence of HSPs (50 µg/mL). The reaction media contained 50 mM of Tris-HCl buffer (pH 7.4), rat liver microsomes 0.5 mg/mL of RLM, magnesium chloride (40 mM) and ATS (0.4 µM) with and without HSPs (50 µg/mL, final concentration)[13]. Preincubate at 37°C for 5 min on shaking water bath. NADPH (1 mM) used as a cofactor was added to initiate the reaction. Sample (100 µL) was withdrawn at 0, 5, 15, 30, 45, and 60 min intervals. Ice-cold ACN (200 µL) containing IS was added to stop the reaction, vortexed (5 min), and centrifuged at 10000 rpm (10 min). 100 µL supernatant was taken for analysis. Microsomes activity was asses by using the positive controls (Testosterone (25 µM). 0 min time interval samples peak area ratio considered as 100% for calculating the % remaining of ATS at different time intervals. The depletion rate constant (k) was calculated by fitting the time vs. % remaining of ATS data into the one-phase decay model with the help of the nonlinear regression analysis module of GraphPad Prism version 7. *In vitro* disappearance $t_{1/2}$ (half-life) and CL_{int} intrinsic clearance for ATS with and without HSPs was calculated by using the following equation[13]:

$$t_{1/2} = \frac{0.693}{k}$$

$$CL_{int} = k * \frac{\text{Volume of reaction mixture}}{\text{mg of protein per reaction}}$$

Effect of HSPs on the pharmacokinetics of ATS

Effect of HSPs on the Pharmacokinetics of ATS was performed in SD rats (200±20 g body weight). Rats were divided into three groups (n=6): Group I: administered ATS (10 mg/kg) alone[14]; while Group II: administered ATS with HSP1 (200 mg/kg); Group III: administered ATS with HSP2 (165 mg/kg) orally. Approximately 300 µL of blood samples were taken at 0.25, 0.5, 1, 2, 4, 8, 12, 24, 48, and 72 h after post-dosing, through retro-orbital plexus into the eppendorf tube containing Sod. EDTA, centrifuged the blood samples for 10 min at 6000 rpm. The collected plasma was stored at -80ºC for further analysis. Plasma samples were proceeded and analyzed as mentioned above. Phoenix 6.3 (Pharsight, Mountain View, CA) software was used to calculate the PK parameters by a non-compartmental analysis model. Relative bioavailability (Fr) was calculated by using the formula:

$$Relative\ bioavailability\ (Fr, \%) = \frac{AUC_{(Combination\ )}}{AUC_{(Alone\ )}} * 100$$

Effect of HSPs on human liver microsomes

The LC-MS/MS methods were developed for simultaneous metabolite quantification as previously published[15]. The CYP isoforms specific probe substrate concentrations were selected as per the USFDA guideline as well as reported in the literature[16-18]. Primary stocks of each probe substrate were prepared by dissolving their respective solvent. Phenacetin, testosterone and diclofenac were dissolved in methanol, coumarin and chlorzoxazone in ACN, dextromethorphan, bupropion, paclitaxel and omeprazole were dissolved in DMSO. Required concentration was obtained by serial dilution in trisbuffer (50 mM, 7.4 pH). The effect of HSPs on human CYP isoforms was determined in the concentration range (1-300 µg/mL). 150 µL reaction media (n=3) contained 0.5 mg/mL of HLM, 50 mM of Tris-HCl buffer (pH 7.4), 40 mM of magnesium chloride, substrates cocktail with and without HSPs (1-300 µg/mL) was pre-incubated at 37ºC for 10 min. The reaction was initiated by adding the cofactor NADPH (1 mM) and incubated at 37ºC for 30 min. Ice cold ACN (200 µL, contains IS1 and IS2) was used to terminate the enzymatic reaction (100 µL sample), vortexed, centrifuged and 100 µL supernatant was taken, and 10 µL was injected for quantification. An equivalent amount of vehicle solvent was added to the control sample with respect to the stock of HSPs. Percent (%) control activity was determined by comparing the metabolite formation in the absence or presence of the HSPs. The IC_{50} values of HSPs for specific CYP isoenzymes were determined using GraphPad Prism 7 software by plotting the logarithm of the inhibitor concentration vs. % control activity remaining after inhibition[15].

Effect of HSPs on the pharmacodynamics of ATS

Male Golden Syrian hamsters (100±10 g) were used to develop the hyperlipidemia model induced by HFD (60% kcal). Hamsters were divided into seven groups (n=6). The treatment dose was selected on the

basis of rat dose. Standard chow diet was fed to the control group. Other groups such as HFD (disease) control, ATS (12 mg/kg), HSP1 (250 mg/kg), a combination of ATS+HSP1, HSP2 (200 mg/kg), and a combination of ATS+HSP2 treated groups were fed with HFDfor 21 days. After one week of HFD feeding, groups 3 to 7 were administered their respective dose for 14 days. Drugs were suspended in the solution of sodium carboxyl methylcellulose (0.5% w/v) and administered orally. Following treatment, animals were fasted overnight, euthanized, and blood and tissue samples were collected. The serum was separated by centrifugation, and all samples were stored at -80±2ºC for further studies.

Fat content estimation

Fat content was estimated by Echo MRI (E26-226-RM Echo MRI LLC, USA) by applying radiofrequency pulses at a distinct static magnetic field described by Taicher *et al.*[19] Each hamster was placed into the plastic cylinder (3 mm thick, 6.8 cm inner diameter) and allowing only limited movement (vertical and horizontal)[19].

Determination of serum lipid profile

Triglyceride (TG), high-density lipoprotein (HDL-C), and low-density lipoprotein (LDL-C) levels were estimated using Erba Mannheim (ErbaLachemas.r.o. Karasek) assay kits. Very low-density lipoprotein (VLDL)[20] levels were calculated using the previously established formula: VLDL (mg/dL) = TG*0.2 and total cholesterol (TC)[21,22] was determined by using the formula: TC (mg/dL) = VLDL+HDL+LDL.

Estimation of oxidative stress parameters

Oxidative parameters in terms of hepatic superoxide dismutase (SOD), catalase (CAT), glutathione (GSH), and malonaldehyde (MDA) were determined as per the reported methods[23].

Measurement of inflammatory cytokines

Hamster IL1β and IL6 ELISA kits (Fine Test) were used to estimate the level of IL1β and IL6 in serum following the manufacturer's protocol.

Real time-PCR

The total RNA was extracted from the liver tissue by the TRIzol method and quantified using NanoDrop-2000 Spectrophotometers (Thermo Fisher Scientific, Waltham, USA). The RNA was reverse transcribed into cDNA using the high-capacity cDNA Reverse Transcription kit and Sure-Cycler 8800 (Agilent Technologies, USA). For cDNA preparation, the reaction condition was programmed as 25ºC for 10 min, 37ºC for 120 min, 85ºC for 5 min, and held at 4ºC. DyNAmoColor Flash SYBR Green qPCR Kit was used for real-time PCR (RT-PCR) analysis with the help of RT-PCR LightCycler 480 Instrument II (Roche Life Science). The reaction conditions were set for RT-PCR analysis at 95ºC for 7 s, 40 cycles comprising 95ºC for 10 s, 60ºC for 15 s and 72ºC for 15 s. The relative mRNA expressions were calculated by using the Ct values. The primers sequence used in this study is comprised in Table 2.

Statistics

Results were expressed as mean ± SD. One-way ANOVA followed by a Newman-Keuls multiple comparisons tests were used for comparison *via.*, GraphPad Prism 7.0 software (GraphPad Software, San Diego, CA, USA). A two-tailed unpaired student t-test was used for comparing data of two groups. $p < 0.05$ value was set as statistically significant. *p<0.05, **p<0.01 and ***p<0.001.

Results and Discussion

Method development

ATS was quantified by using LC-MS/MS (API QTRAP 4000). Initially, fragmentations of ATS and PHEN were performed in both modes. ATS and PHEN showed higher and stable fragment ions in positive ion mode. Source and compounds parameters of ATS and PHEN are listed in Table 1, and MS/MS spectra are depicted in Figure 1. ATS and PHEN were quantified in positive ion mode. Then, chromatographic separation was performed by using the Shimadzu UFLC system. Several mobile phases

Table 2 — Sequence of oligonucleotides used as a primer for real-time quantitative qRT-PCR

Gene	Forward sequence (5' to 3')	Reverse sequence (5' to 3')
haHMGCR	GGCCCCACATTTACCCTTGA	CTGGCAAAATGGCTGAGCTG
haCYP7A1	CACTCTGCACCTTGAGGATGG	GGGTCTGGGTAGATTGCAGG
haLXRα	TCAGCATCTTCTCTGCAGACCGG	TCATTAGCATCCGTGGGAACA
haSREBP1c	ATGGACGAGCTGGCCTTCGGTGAGGCGGC	CAGGAAGGCTTCCAGAGAGGA
haβ-Actin	TGCTGTCCCTGTATGCCTCTG	AGGGAGAGCGTAGCCCTCAT

*ha= Hamster

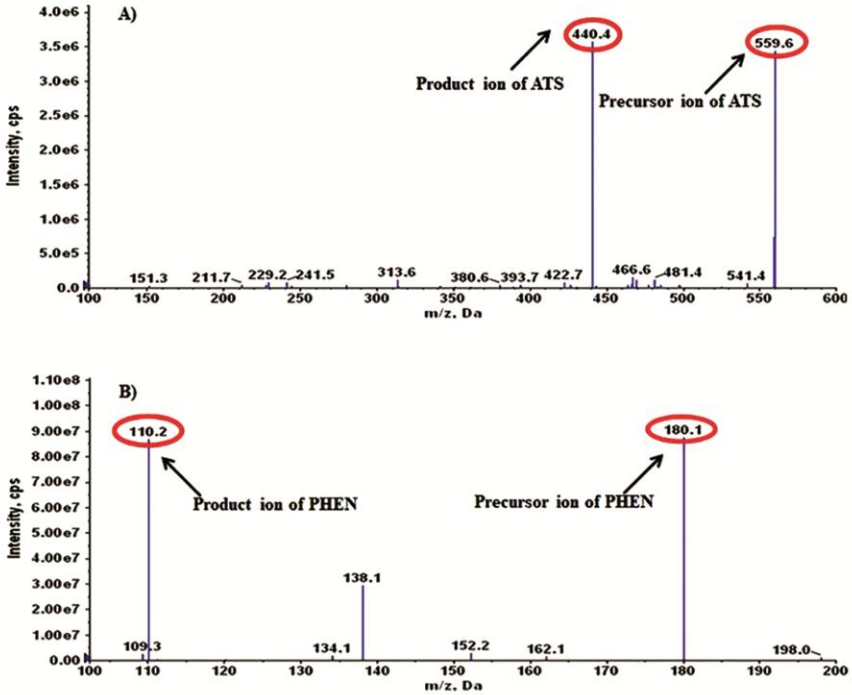

Fig. 1 — MS/MS spectra of precursor ion to selected product ion transition of (A) ATS and (B) PHEN (IS)

and many columns were tried for chromatographic separation. Finally, 0.1% formic acid in ACN and ammonium acetate (10 mM) was found to be a suitable mobile phase in the composition of 80:20 v/v for elution of ATS and PHEN. Phenomenex Luna column (C18 (2), 100A, 7.5 x 4.6 mm, 3 µ) was showed a sharp and high intense peak with a shorter run time (5 min). ATS and PHEN were eluted at a flow rate of 0.4 mL/min. Internal standards (PHEN, IS) were selected based on several similarities like ionization efficiency, chromatographic retention and extraction behaviours of ATS. 10 µL samples were injected for quantification.

Extraction recovery and matrix effect

Two-step procedures (PPT followed by LLE) were applied to extract ATS from the rat plasma. PPT followed by LLE provided a clear sample, good recovery and minimized the matrix effect. ACN and mixture of EA:TBME (50:50) were found to be suitable for extraction of ATS. The recovery of ATS at LQC, MQC and HQC levels were found to be 86.06±3.55, 93.44±3.63, 93.02±3.35%, respectively and the matrix effects at the same QCs levels were recorded as 0.93±0.01, 0.96±0.02, and 0.94±0.06, respectively.

Bioanalytical method validation

The LC-MS/MS bioanalytical ATS method was validated according to the USFDA guideline. The liquid chromatographic condition confirmed that the ATS and PHEN were reproducible. The retention time (RT) of ATS and PHEN was 2.73 min and 2.38 min, respectively. The CS linearity (r^2) was > 0.995 (n=3) and the acceptance criteria were within the range limits. The extraction method was specific because no interference was observed in the matrix plasma at the RT of ATS and PHEN (Fig. 2). Intra and inter-day accuracy and precision were performed at four different QCs levels and manifested in Table 3. ATS precision and accuracy were within acceptable limits. No carryover was found in blank plasma samples after sample injection of 500 ng/mL.

Effect of HSPs on intestinal permeability of ATS

Both P-gp, as well as CYP450 enzymes, are expressed in the intestine. P-gp inhibitors or CPY450 inhibitors enhance the bioavailability of the orally administered drug by inhibiting intestinal efflux transport and decreasing the first-pass intestinal or hepatic metabolism. Keeping this perspective, westudied the effect of HSP1 and HSP2 on the intestinal permeability of ATS. ATS was perfused alone or along with HSP1 or HSP2 to assess the intestinal permeability of ATS by using the *in situ* single-pass intestinal perfusion (SPIP) model. SPIP study was performed as per previously developed method with some modification. The effective

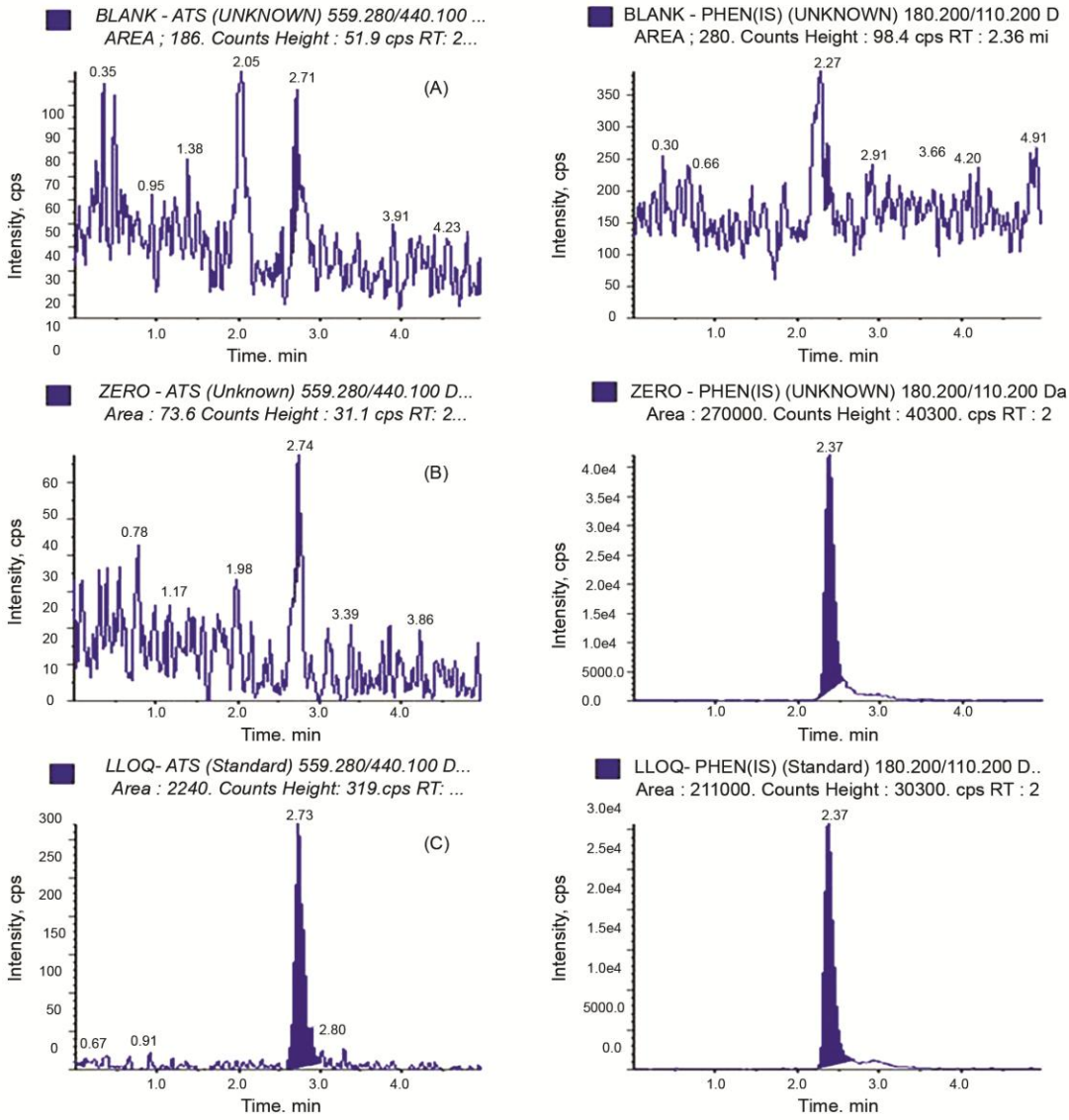

Fig. 2 — MRM chromatogram of analytes in rat plasma (n=6). (A) blank plasma (without ATS and IS), (B) zero sample (only IS, PHEN) for ATS, and (C) plasma spiked with LLOQ (1 ng/mL) of ATS and IS)

Table 3 — Precision and accuracy of ATS in rat plasma (n=6, mean ± SD)

Analyte	Level	Nominal Conc (ng/mL)	Intra-day			Inter day		
			Obs. Conc (ng/mL)	Precision (%)	Accuracy (%)	Obs. Conc (ng/mL)	Precision (%)	Accuracy (%)
ATS	LLOQ	1	0.87 ± 0.06	6.73	87.18	0.92 ± 0.06	6.31	91.93
	LQC	3	3.23 ± 0.17	5.24	107.72	3.10 ± 0.18	5.91	103.46
	MQC	189	199.50 ± 8.22	4.12	105.83	201.33 ± 9.73	4.83	106.65
	HQC	375	412.33 ± 19.3	4.69	109.93	399.17 ± 16.87	4.18	106.44

permeability (P_{eff}) of ATS perfused alone or in combination with HSP1 and or HSP2 were found to be 0.00159±0.00015 cm/s for ATS alone, 0.00326±0.00061** cm/s for ATS+HSP1 and 0.00202±0.00017* cm/s for ATS+HSP2. The permeability of ATS was significantly enhanced when perfused with HSP1 and/ HSP2.

Effect of HSPs on the metabolism of ATS

Liver microsomes are sub-cellular fractions that contain several enzymes responsible for the

metabolism of various drugs, e.g., cytochrome P450s (CYPs), carboxylesterases, flavin monooxygenases and epoxide hydrolase. The effect of HSP1 or HSP2 on the metabolism of ATS by CYP450 enzymes was investigated in RLM. Testosterone was used as a positive control for phase-I reaction-based metabolism to assess the enzyme activity. Our results show that the metabolism of ATS (0.4 µM) was affected due to HSPs (50 µg/mL). In addition, HSPs significantly inhibited the *in vitro* metabolism of ATS (Fig. 3A). Moreover, the combination groups have a significant inhibition effect, *i.e*., on the *in vitro* $t_{1/2}$ and CL_{int} compared to ATS alone (Table 4).

Effect of HSPs on the human CYPs isoform

Enzyme inhibition kinetics parameters, *i.e*., IC_{50} (concentration of an inhibitor that caused 50% of inhibition), used for metabolism-based DIs, are important kinetic parameters for predicting mechanism-based DIs[24]. The data will help to understand and address the potential of drug interaction studies. From this perspective, *in vitro* metabolism studies play a key role in identifying metabolic pathways and predicting DIs. Potent inhibition or induction of CYP isoenzymes such as CYP1A2, CYP2A6, CYP3A4, CYP2B6, CYP2C8, CYP2C9, CYP2C19, and CYP2D6 may give rise to safety issues and clinical DIs[25]. The effect of HSP1 or HSP2 on the CYP enzymes was investigated through in vitro inhibition assay by using human liver microsomes. HSP1 has shown inhibitory effects on human CYP isoforms, *i.e*., CYP1A2, 2B6, 2C9, 2C19, 2D6, 2E1, and CYP3A4. The IC_{50} values of HSPs are listed in Table 5. CYP1A2-catalyzed phenacetin O-deethylation, 2A6-catalyzed coumarin 7-hydroxylation, 2B6-catalyzed bupropion 6-hydroxylation, 2C8-catalyzed paclitaxel -6α-hydroxylation, 2C9-catalyzed diclofenac 4'-hydroxylation, 2C19-catalyzed omeprazole 5-hydroxylation, 2D6- catalyzedO-demethylation of dextromethorphan to dextrorphan, 2E1-catalyzed chlorzoxazone 6-hydroxylation and 3A4- catalyzed testosterone 6β-hydroxylation activities.

The CYP3A4 based conversion of the testosterone into 6-*β*-hydroxy testosterone was inhibited by the HSP2. It is predicted that the drugs metabolized by these CYP enzymes are prone to herb-drug interaction when administered with HSP1 (inhibited CYP1A2, 2B6, 2C9, 2C19, 2D6, 2E1, and CYP3A4) and HSP2 (inhibited CYP3A4).The *in-vitro* inhibition levels of plant extract against the human CYPs, *i.e.*, weak, moderate, and potent inhibition, are categorized based on IC_{50} values. The plant extract is constituted as a weak, medium and potent inhibitor against human CYPs isoforms if the IC_{50} values are in the range of 100-200 µg/mL, 10–99.9 µg/mL and ≤9.9 µg/mL, respectively[15]. CYP450 enzymes were inhibited by

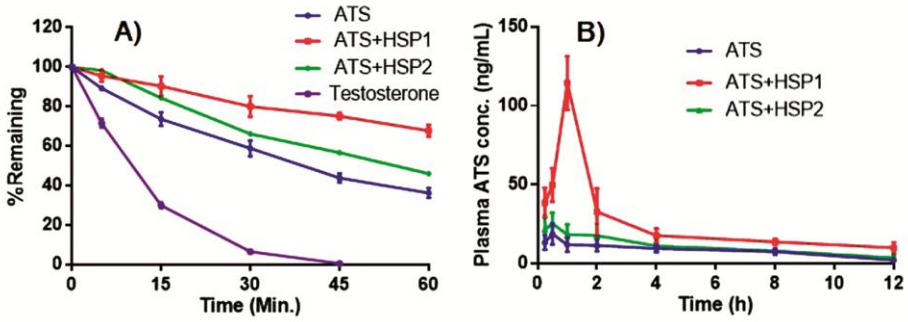

Fig. 3 —Microsomal stability studies (n=3) of (A) ATS (0.4 µM) with and without HSPs (50 µg/mL). Testosterone (25 µM) was used as a positive control to assess the microsomes activity; Plasma PK profile of (B) ATS (10 mg/kg) co-administered with and without HSP1 (200 mg/kg) and HSP2 (165 mg/kg) orally. Values are represented as mean ± SD (n=6)

Table 4 — Effect of HSPs on the in vitro $t_{1/2}$, and CL_{int} of ATS (mean ± SD, n=3)

Parameters (unit)	ATS	ATS+HSP1	ATS+HSP2
Depletion rate constant (k, 1/min)	0.02257±0.00147	0.00908±0.0009**	0.01371±0.00034*
In vitro half life ($t_{1/2}$, min)	30.80±1.94	76.85±7.75**	50.58±1.23*
In vitro intrinsic clearance (CL_{int}, µL/min/mg)	45.13±2.93	18.16±1.79**	27.41±0.67*

*=p<0.05 and **=p<0.01.

Table 5 — Effect of HSPs on human CYP isoform-specific metabolite formation

Substrate (Conc. μM)	Human CYP isoform (metabolite)	HSP1 IC50 (μg/mL)	HSP2 IC50 (μg/mL)
Phenacetin (50)	1A2 (Acetaminophen)	126.1	>200
Coumarin (5)	2A6 (7-hydroxycoumarin)	>200	>200
Bupropion (50)	2B6 (6-hydroxybupropion)	83.2	>200
Paclitaxel (10)	2C8 (6α-hydroxypaclitaxel)	>200	>200
Diclofenac (5)	2C9 (4'-hydroxydiclofenac)	127.9	>200
Omeprazole (20)	2C19 (5-hydroxyomeprazole)	105.7	>200
Dextromethorphan (5)	2D6 (Dextrorphan)	123.5	>200
Chlorzoxazone (50)	2E1 (6-hydroxychlorzoxazone)	110	>200
Testosterone (25)	3A4 (6β-hydroxytestosterone)	149.6	105.4

Table 6 — Effect of HSPs on the pharmacokinetic parameters of ATS (n=6, mean ± SD)

Parameter (Unit)	ATS	ATS in ATS+HSP1 Group (Mean ± SD)	ATS in ATS+HSP2 Group (Mean ± SD)
C_{max} (ng/mL)	19.07±6.31	114.4±17.07	27.90±5.94
$AUC_{0-\infty}$ (h*ng/mL)	109.12±26.83	317.6±53.16	146.99±27.89
T_{max} (h)	0.46±0.10	1	0.42±0.13
$T_{1/2}$ (h)	3.59±0.54	3.79±0.8	3.94±1.18
CL/F (L/hr/Kg)	95.94±21.42	27.41±4.19	70.21±14.03
Vd/F (L/Kg)	484.91±62.05	148.52±33.25	405.88±161.45
MRT (h)	5.75±0.64	6.32±0.59	6.20±1.06
% Fr		347.87±42.87	136.13±10.30

T. chebula extract[26]. It has been reported that *Garcinia cambogia* interacts with antidiabetic drugs, antidepressants and HMG CoA reductase inhibitors. It also inhibited the CYP 2B6 and modulated the PK profiles of CYP2B6 substrate drugs[27]. *Guggulsterone* inhibited the CYP3A4[28], *Trigonellafoenum-graecum* inhibited the CYP2D gene expression[29].

Effect of HSPs on the pharmacokinetics of ATS

The pharmacokinetic profiles of ATS concomitantly administered with and without HSPs in SD rats are shown in Fig. 3B. HSPs altered the pharmacokinetic parameters of ATS. Administration of ATS along with HSPs has increased the relative bioavailability of ATS with respect to the group administered alone. The relative bioavailability of ATS was increased due to an increase in absorption and/or decreased first-pass intestinal or hepatic metabolism. The pharmacokinetic parameters of ATS co-administered with and without HSPs are listed in Table 6. The bioavailability of ATS was increased in the combination group may be due to inhibition of ATS metabolism and enhancement of ATS permeability. CYP3A4 is responsible for the metabolism of orally administered ATS (HMG-CoA reductase inhibitor)[30].

Effect of HSPs on the pharmacodynamics of ATS

Golden Syrian hamsters are commonly used to induce hyperlipidemia by excessive dietary cholesterol intake. Fat content was estimated by using the Echo MRI method. Exposure to HFD increases the fat content (HFD vs. control). Treatment of ATS, HSP1, ATS+HSP1, HSP2, and ATS+HSP2 significantly reduced the fat content (HFD vs. treatments). Co-administration of HSPs with ATS significantly reduced the fat content with respect to ATS and HSPs alone treated groups (Fig. 4A). Excess chronic production of inflammatory cytokines is responsible for inflammatory diseases. T helper cells and macrophages produce the inflammatory cytokines and upregulate the inflammatory reactions[31]. IL1β and IL6 levels were increased in HFD group and restored upon treatments. Combinations and alone treatment groups significantly inhibited the excess production of IL1 (Fig. 4B) and IL6 (Fig. 4C) levels (upregulated by HFD). Polyunsaturated fatty acid's peroxidation causes an increase in free radicals, responsible for the chronic production of MDA[32]. End product of lipid peroxidation, *i.e.*, MDA levelswere significantly increased in the HFD group and decreased after treatment. SOD catalyzes the dismutation of superoxide anion to hydrogen peroxide via GSH or CAT, subsequently converting it into water and oxygen[33]. Under physiological conditions, H_2O_2 is detoxified by the catalase enzyme. The SOD, CAT and GSH activities were decreased in the disease control (HFD fed) group with respect to the control group (fed with standard diet) and restored

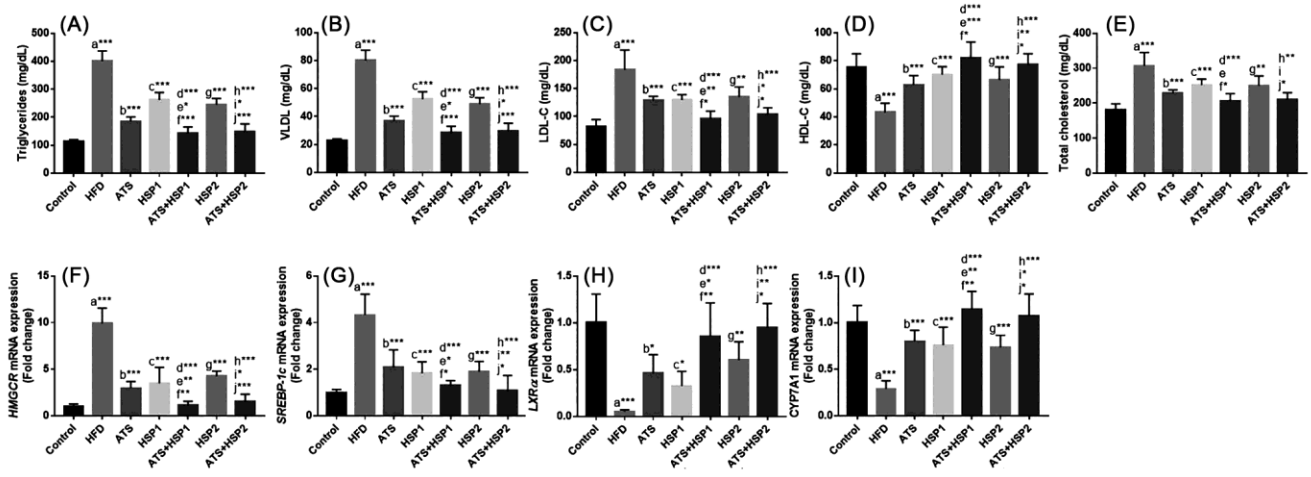

Fig. 4 — Estimation of (A) fat content, (B) IL1β, (C) IL6, (D) tissue MDA, (E) GSH, (F) SOD, and (G) CAT levels in Hamster. a: represent comparison between control vs HFD; b: represent HFD vs ATS treatment; c: represent HFD vs HSP1 treatment; d: represent HFD vs ATS+HSP1 treatment; e: ATS treatment vs ATS+HSP1 treatment; f: HSP1 treatment vs ATS+HSP1 treatment; g: represent HFD vs HSP2 treatment; h: represent HFD vs ATS+HSP2 treatment; i: ATS treatment vs ATS+HSP2 treatment; j: HSP2 treatment vs ATS+HSP 2 treatment. Values are represented as Mean ± SD (n = 6)

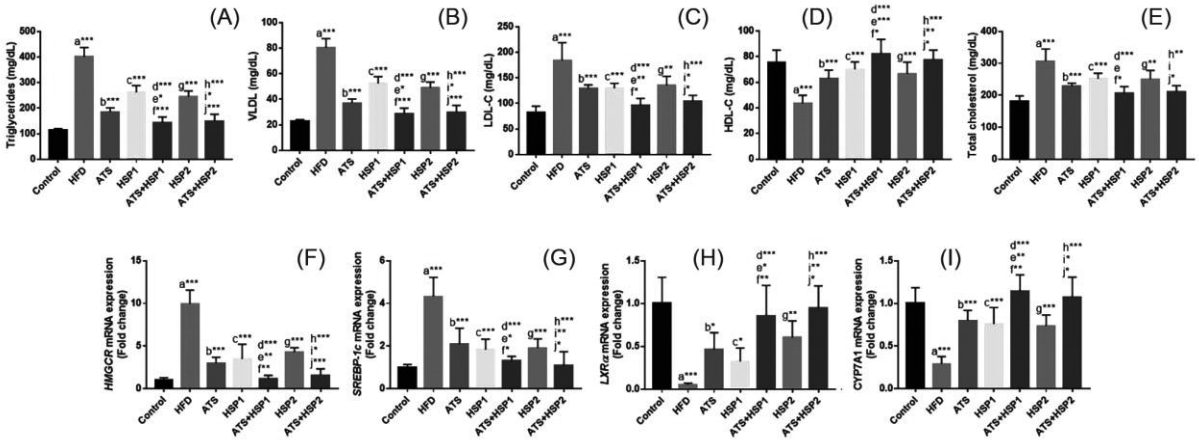

Fig. 5 — Effects on lipid profiles (A) TG, (B) VLDL, (C) LDL, (D) HDL, and (E) TC; mRNA expression levels of (F) HMGCR, (G) SREBP1c, (H) LXRα, and (I) CYP7A1. a: represent comparison between control vs HFD; b: represent HFD vs ATS treatment; c: represent HFD vs HSP1 treatment; d: represent HFD vs ATS+HSP1 treatment; e: ATS treatment vs ATS+HSP1 treatment; f: HSP1 treatment vs ATS+HSP1 treatment; g: represent HFD vs HSP2 treatment; h: represent HFD vs ATS+HSP2 treatment; i: ATS treatment vs ATS+HSP2 treatment; j: HSP2 treatment vs ATS+HSP2 treatment. Values are represented as Mean ± SD

upontreatment. Combinations and alone treatment groups significantly inhibited the tissue MDA level (upregulated by HFD) and upregulated the SOD, CAT, and GHS levels (Fig. 4D-G).

HFD altered the lipid profiles. Lipid levels, *i.e.*, TG, LDL, VLDL and TC levels, were increased in the HFD group and significantly inhibited its elevation after treatment. The combination of ATS+HSP1 and ATS+HSP2 significantly reduced the TG, LDL, VLDL, TC levels (Fig. 5A-E). Conversion of HMG-CoA to mevalonic acid catalyzed by HMGCR subsequently synthesizes cholesterol. The induction of SREBP1[34] activated the transcription of the HMGCR gene[35] and finally increased cholesterol production. Circulatory cholesterol is removed in the form of bile acid by activation of PPARα[36]. Activation of LXRα[37] regulated the lipid-controlling gene, reversed the cholesterol transport and decreased lipid accumulation. CYP 7A1[37] has played an essential role in cholesterol metabolism. It converts cholesterol into bile acid. HMGCR and SREBP1c mRNA expression levels were significantly increased upon exposure to HFD and decreased across treatments. The LXRα and CYP7A1 mRNA

expression levels were down regulated in HFD group and upregulated by treatments. The coadministration of ATS either with HSP1 or HSP2 significantly inhibited the HMGCR and SREBP1c upregulation and led to significant increase in the production of LXRα and CYP7A1 mRNA expression levels with respect to the alone treatment group (Fig. 5F-I). In addition, a significant effect was found when ATS was administered concomitantly with HSPs. The above finding suggests that dose adjustment should be required when taking ATS (atorvastatin) with HSPs. ATS and HSPs co-administration may result in more adverse events.

Conclusions

The above finding concluded that the HSPs enhanced the permeability and inhibited the *in vitro* metabolism of ATS. Co-administration of HSPs with ATS has increased the ATS relative bioavailability. The combination of ATS+HSPs significantly reduced the fat content, inflammatory cytokines, tissue MDA, TG, LDL, VLDL, TC levels, HMCR, SREBP1 mRNA expression and improved the production of HDL level, tissue SOD, CAT, GSH, LXRα and CYP 7A1 mRNA expression levels compared with alone treatment groups.The above finding suggested that precaution should be taken when both ATS and HSPs will be administered concomitantly, as this could lead to potential interactions.

Acknowledgements

AH, RK and SAA are thankful to ICMR for the research fellowships;SV is grateful to CSIR. MIR, SK, AK and SDD are thankful to DST; PS is thankful to UGC. JRG is thankful to DBT and CSIR for financial support. CDRI communication number: 125/2021/JRG.

Conflict of Interest

Authors should declare no competing or conflict of interest.

Author's Contributions

AH and JRG designed the current research experiments. AH, MIR, SDD, SAA, PS, SV, RK, and AK performed the experiments. AH and JRG wrote and edited the manuscript.

References

1 Anderson L L, Berns E J, Bugga P, George Jr A L & Mrksich M, Measuring drug metabolism kinetics and drug–drug interactions using self-assembled monolayers for matrix-assisted laser desorption-ionization mass spectrometry, *Anal Chem*, 88 (17) (2016) 8604-8609, DOI: 10.1021/acs.analchem.6b01750.

2 Pontelo B M, Greco D B, Guimarães N S, Rotsen N, Braga V A R, *et al*., Profile of drug-drug interactions and impact on the effectiveness of antiretroviral therapy among patients living with HIV followed at an Infectious Diseases Referral Center in Belo Horizonte, Brazil, *Braz J Infect Dis*, 24 (2) (2020) 104-109, DOI: 10.1016/j.bjid.2020.03.006.

3 Wójcikowski J, Danek P J, Basińska-Ziobroń A, Pukło R & Daniel W A, In vitro inhibition of human cytochrome P450 enzymes by the novel atypical antipsychotic drug asenapine: a prediction of possible drug–drug interactions, *Pharmacol Rep*, 72 (3) (2020) 612-621, DOI: 10.1007/s43440-020-00089-z.

4 Hoyos P, Pace V & Alcántara A R, Biocatalyzed synthesis of statins: A sustainable strategy for the preparation of valuable drugs, *Catalysts*, 9 (3) (2019) 260, DOI: 10.3390/catal9030260.

5 Husain A, Kaushik A, Awasthi H, Singh D P, Khan R, *et al*., Immunomodulatory and antioxidant activities of fresh juice extracts of Brahmi and Guduchi, *Indian J Tradit Know*, 16 (3) (2017) 498-505, DOI: 6 Kahraman C, Arituluk Z C & Cankaya I I T, The clinical importance of herb-drug interactions and toxicological risks of plants and herbal products, In: *Medical Toxicology*, Pınar Erkekoglu and Tomohisa Ogawa (Eds), IntechOpen, 2021. doi: 10.5772/intechopen.92040

7 Balkrishna A, Solleti S K, Singh H, Verma S, Sharma N, *et al*., Herbal decoction Divya-Swasari-Kwath attenuates airway inflammation and remodeling through Nrf-2 mediated antioxidant lung defence in mouse model of allergic asthma, *Phytomedicine*, 78 (2020) 153295, DOI: 10.1016/j.phymed.2020.153295.

8 FDA US, Bioanalytical method validation. Guidance for industry, US Department of Health and Human Services, *US FDA, Cent Drug Eval Res Cent Biol Eval Res Cent Vet Med*, 2018, DOI: https://www.fda.gov/files/drugs/published/Bioanalytical-Method-Validation-Guidance-for-Industry.pdf.

9 Riyazuddin M, Husain A, Verma S, Katekar R, Garg R, *et al*., Simultaneous quantification of five biomarkers in ethanolic extract of: Cassia occidentalis Linn, stem using liquid chromatography tandem mass spectrometry: Application to its pharmacokinetic studies, *RSC Adv*, 10 (8) (2020) 4579-4588, DOI: 10.1039/c9ra07482a.

10 Wahajuddin, Singh S P, Raju K S R, Nafis A & Jain G K, Simultaneous determination of nine model compounds in permeability samples using RP-HPLC: Application to prove the cassette administration principle in single pass intestinal perfusion study in rats, *J Pharm Biomed Anal*, 67 (2012) 71-76, DOI: 10.1016/j.jpba.2012.03.048.

11 Riyazuddin M, Husain A, Valicherla G R, Verma S, Gupta A P, *et al*., Development and validation of LC-MS/MS method for quantification of novel PP2A – β-catenin signalling inhibitor, S011-2111 in mice plasma: Application to its preclinical pharmacokinetic studies, *J Chromatogr B: Anal Technol Biomed Life Sci*, 1130-1131 (2019), DOI: 10.1016/j.jchromb.2019.121829.

12 Chhonker Y S, Chandasana H, Mukkavilli R, Prasad Y D, Laxman T S, *et al*., Assessment of *in vitro* metabolic stability, plasma protein binding, and pharmacokinetics of E-and

Z-guggulsterone in rat, *Drug Test Anal*, 8 (9) (2016) 966-975, DOI: 10.1002/dta.1885.

13 Riyazuddin M, Valicherla G R, Husain A, Hussain M K, Shukla M, *et al*., Elucidation of pharmacokinetics of novel DNA ligase I inhibitor, S012-1332 in rats: Integration of *in vitro* and *in vivo* findings, *J Pharm Biomed Anal*, 162 (2019) 205-214, DOI: 10.1016/j.jpba.2018.09.031.

14 Vijayakumar R & Nachiappan V, Cassia auriculata flower extract attenuates hyperlipidemia in male Wistar rats by regulating the hepatic cholesterol metabolism, *Biomed Pharmacother*, 95 (2017) 394-401, DOI: 10.1016/j.biopha. 2017.08.075.

15 Husain A, Riyazuddin M, Katekar R, Verma S, Syed A A, *et al*., Herb–drug interaction studies of ethanolic extract of Cassia occidentalis L. coadministered with acetaminophen, theophylline, omeprazole, methotrexate and methylprednisolone, *Phytomed Plus*, 1 (1) (2021) 100008, DOI: 10.1016/j.phyplu.2020.100008.

16 FDA US, Drug Interactions & Labeling-Drug Development and Drug Interactions: Table of Substrates, Inhibitors and Inducers, 2017.

17 Valicherla G R, Mishra A, Lenkalapelly S, Jillela B, Francis F M, *et al*., Investigation of the inhibition of eight major human cytochrome P450 isozymes by a probe substrate cocktail in vitro with emphasis on CYP2E1, *Xenobiotica*, 49 (12) (2019) 1396-1402, DOI: 10.1080/00498254.2019.1581301.

18 Yu J S, Choi M S, Park J S, Rehman S U, Nakamura K, *et al*., Inhibitory effects of Garcinia cambogia extract on CYP2B6 enzyme activity, *Planta Med*, 83 (11) (2017) 895-900, DOI: 10.1055/s-0043-104934.

19 Taicher G Z, Tinsley F C, Reiderman A & Heiman M L, Quantitative magnetic resonance (QMR) method for bone and whole-body-composition analysis, *Anal Bioanal Chem*, 377 (6) (2003) 990-1002, DOI: 10.1007/s00216-003-2224-3.

20 Valicherla G R, Gupta A P, Hossain Z, Riyazuddin M, Syed A A, *et al*., Pancreastatin inhibitor, PSTi8 ameliorates metabolic health by modulating AKT/GSK-3β and PKCλ/ζ/SREBP1c pathways in high fat diet induced insulin resistance in peri-/ post-menopausal rats, *Peptides*, 120 (2019), DOI: 10.1016/ j.peptides.2019.170147.

21 Sampson M, Ling C, Sun Q, Harb R, Ashmaig M, *et al*., A new equation for calculation of low-density lipoprotein cholesterol in patients with normolipidemia and/or hypertriglyceridemia, *JAMA Cardiol*, 5 (5) (2020) 540-548, DOI: 10.1001/jamacardio.2020.0013.

22 Sathiyakumar V, Blumenthal R & Elshazly M B, New information on accuracy of LDL-C estimation, *Am Coll Cardiol*, 2020.

23 Rawat A, Chaturvedi S, Singh A K, Guleria A, Dubey D, *et al*., Metabolomics approach discriminates toxicity index of pyrazinamide and its metabolic products, pyrazinoic acid and 5-hydroxy pyrazinoic acid, *Hum Exp Toxicol*, 37 (4) (2018) 373-389, DOI: 10.1177/0960327117705426.

24 Baranczewski P, Stanczak A, Sundberg K, Svensson R, Wallin A, *et al*., Introduction to in vitro estimation of metabolic stability and drug interactions of new chemical entities in drug discovery and development, *Pharmacol Rep*, 58 (4) (2006) 453.

25 Zhang D, Zhu M & Humphreys W G, Drug metabolism in drug design and development: Basic concepts and practice, (John Wiley & Sons), 2007.

26 Ponnusankar S, Pandit S, Venkatesh M, Bandyopadhyay A & Mukherjee P K, Cytochrome P450 inhibition assay for standardized extract of Terminalia chebula Retz, *Phytother Res*, 25 (1) (2011) 151-154, DOI: 10.1002/ptr.2993.

27 Barrea L, Altieri B, Polese B, De Conno B, Muscogiuri G, *et al*., Nutritionist and obesity: Brief overview on efficacy, safety, and drug interactions of the main weight-loss dietary supplements, *Int J Obes Suppl*, 9 (1) (2019) 32-49, DOI: 10.1038/s41367-019-0007-3.

28 Sabarathinam S, Chandra S K R & Mahalingam V T, CYP3A4 mediated pharmacokinetics drug interaction potential of Maha-Yogaraj Gugglu and E, Z guggulsterone, *Sci Rep*, 11 (1) (2021) 1-8, DOI: 10.1038/s41598-020-80595-5.

29 Al-Jenoobi F I, Korashy H M, Ahad A, Raish M, Al-Mohizea A M, *et al*., Potential inhibitory effect of herbal medicines on rat hepatic cytochrome P450 2D gene expression and metabolic activity, *Pharmazie*, 69 (11) (2014) 799-803, DOI: 10.1691/ph.2014.4651.

30 Lins R L, Matthys K E, Verpooten G A, Peeters P C, Dratwa M, *et al*., Pharmacokinetics of atorvastatin and its metabolites after single and multiple dosing in hypercholesterolaemic haemodialysis patients, *Nephrol Dial Transplant*, 18 (5) (2003) 967-976, DOI: 10.1093/ndt/gfg048.

31 Kaneko N, Kurata M, Yamamoto T, Morikawa S & Masumoto J, The role of interleukin-1 in general pathology, *Inflamm Regen*, 39 (1) (2019) 1-16, DOI: 10.1186/s41232-019-0101-5.

32 Rosa A C, Bruni N, Meineri G, Corsi D, Cavi N, *et al*., Strategies to expand the therapeutic potential of superoxide dismutase by exploiting delivery approaches, *Int J Biol Macromol*, 168 (2021) 846-865, DOI: 10.1016/j.ijbiomac. 2020.11.149.

33 Younus H, Therapeutic potentials of superoxide dismutase, *Int J Health Sci* (*Qassim*), 12 (3) (2018) 88.

34 Bertolio R, Napoletano F, Mano M, Maurer-Stroh S, Fantuz M, *et al*., Sterol regulatory element binding protein 1 couples mechanical cues and lipid metabolism, *Nat Commun*, 10 (1) (2019) 1-11, DOI: 10.1038/s41467-019-09152-7.

35 Jiang S-Y, Li H, Tang J-J, Wang J, Luo J, *et al*., Discovery of a potent HMG-CoA reductase degrader that eliminates statin-induced reductase accumulation and lowers cholesterol, *Nat Commun*, 9 (1) (2018) 1-13, DOI: 10.1038/s41467-018-07590-3.

36 Bougarne N, Weyers B, Desmet S J, Deckers J, Ray D W, *et al*., Molecular actions of PPAR α in lipid metabolism and inflammation, *Endocr Rev*, 39 (5) (2018) 760-802, DOI: 10.1210/er.2018-00064.

37 Chiang J Y L & Ferrell J M, Up to date on cholesterol 7α-hydroxylase (CYP7A1) in bile acid synthesis, *Liver Res*, 4 (2) (2020) 47-63, DOI: 10.1016/j.livres.2020.05.001.